Available online at www.sciencedirect.com
SCIENCE DIRECT
Surface Science 600 (2006) 2070–2078
SURFACE SCIENCE
www.elsevier.com/locate/susc

High-resolution study of quasi-elastic electron scattering from a two-layer system

M.R. Went, M. Vos *

Atomic and Molecular Physics Laboratories, Research School of Physical Sciences and Engineering, The Australian National University, Canberra, ACT 0200, Australia

Received 6 January 2006; accepted for publication 23 February 2006
Available online 20 March 2006

Abstract

In large-angle elastic scattering events of keV electrons a significant amount of momentum is transferred from the electron to a nucleus in the target. As a consequence kinetic energy is transferred from the energetic electron to the nucleus, and hence these processes can be referred to as 'quasi-elastic'. How much energy is transferred depends on the mass of the nucleus. In this paper, we present measurements from a two-layer system (a germanium layer and a carbon layer), and at high energies the quasi-elastic peaks of Ge and C are clearly resolved. It is demonstrated that the sample geometry has a huge effect on the observed relative intensities. It is shown that the intensities are influenced by the elastic scattering cross-section of the atoms in the film, film composition and selective attenuation, due to varying amount of inelastic scattering for layers of the film. However truly quantitative agreement is not obtained.

Keywords: Thin films; Elastic electron scattering; Electron–solid interactions; Scattering; Diffraction; Electron–solid scattering and transmission-elastic; Electron energy loss spectroscopy; Electron–solid interactions; Carbon; Germanium

1. Introduction

Electrons scattering elastically from surfaces have been used to study sample composition of the outermost layer. In this so-called elastic peak electron spectroscopy (EPES) the measured intensity is determined by an interplay between the elastic scattering cross-section and the inelastic mean free path (as inelastic processes remove intensity from the elastic peak) [1]. Indeed by assuming that the elastic scattering processes are understood, the EPES measurements are often used to determine the inelastic mean free path (see e.g. [2,3]).

Since the work of Boersch et al. [4] it is known that there is an energy loss involved in large-angle elastic scattering events, consistent with momentum transfer to a single atom in the scattering event. If an incoming electron with momentum $\mathbf{p}_0$ scatters over an angle θ its momentum changes by a magnitude $q = 2p_0\sin(\theta/2)$. This momentum is transferred to a target atom with mass M. If the target atom is at rest before the collision the recoil energy E_r transferred will be $q^2/2M$.

The recoil energy is conveniently obtained in eV by $E_r = Cq^2/M$ with M in atomic mass units, and $C = 0.00741$ and the momentum transfer q expressed in atomic units ($\hbar = m_e = 1$), or $C = 0.00207$ when the momentum transfer is expressed in Å^{-1} (1 a.u. of momentum $\simeq 1.89\ \text{Å}^{-1}$). Thus the energy loss of a 30 keV electron ($p_0 = 90.02\ \text{Å}^{-1}$) scattered over 45° ($q = 68.9\ \text{Å}^{-1}$) is 9.8 eV for scattering from a proton, 0.81 eV for scattering from C, and 0.14 eV for scattering from a Ge nucleus. Hence good energy resolution is required if one wants to separate Ge from C under these conditions.

If the target atom has a momentum $\mathbf{k}$ *before* the collision (and corresponding kinetic energy $k^2/2M$) the energy transfer is given by:

$$E_r = \frac{(\mathbf{k}+\mathbf{q})^2}{2M} - \frac{k^2}{2M} = \frac{q^2}{2M} + \frac{\mathbf{q}\cdot\mathbf{k}}{M}. \quad (1)$$

* Corresponding author.
E-mail address: maarten.vos@anu.edu.au (M. Vos).

0039-6028/$ - see front matter © 2006 Elsevier B.V. All rights reserved.
doi:10.1016/j.susc.2006.02.038

Thus there is a shift in energy and a Doppler broadening of the elastic peak. For the same scattering angle the shift and broadening decreases with increasing atomic mass. In recent years elastic scattering experiments have confirmed both the shift and broadening convincingly for light and medium mass nuclei. For heavy elements the broadening and shift is still of the order of the experimental resolution. These experiments were done both in reflection [5,6] and in transmission [7]. Especially the contribution of electrons scattered from hydrogen was well resolved from that of carbon in polymer films. The hydrogen peak width in these measurements could not be explained by assuming kT kinetic energy per degree of freedom. Instead it reflects the zero-point motion of the bound hydrogen nucleus in the polymer film [7]. The underlying physics of these scattering experiments is analogous to that of neutron Compton scattering. Indeed consistent results were obtained in a comparative study of neutron and electron scattering experiments of polymer films [8,9].

Here we want to continue this line of research. We improved the energy resolution and now we can resolve carbon signal from that of heavier elements such as germanium. By evaporating germanium on a thin, free-standing carbon film we prepared a target suitable for study in a transmission and reflection geometry. We investigate the influence of measurement geometry on the observed intensities, as well as the dependence of the spectra on the energy of the incoming electrons.

Interpretation of these measurements depends on the elastic differential cross-section and the inelastic mean free path. We give the relevant quantities in Table 1. We calculated inelastic mean free path values using the semi-empirical expression given by Tanuma et al. [10] for electrons with energy E (in eV) and λ (in Å):

$$\lambda \approx E/[E_p^2 \beta \ln(\gamma E)] \tag{2}$$

with E_p the plasmon energy, β and γ tabulated parameters [10]. This formula was developed for XPS energies (up to 2 keV), and the current extrapolation to 30 keV is pushing the limits.

In recent publications rather different values are given for the inelastic mean free path, especially for graphite [11,13]. We reproduce the calculated inelastic mean free path based on the [10 and 11] in Table 1. For Ge an experimental determination at 30 keV gives a value of 350 Å [14], which is in surprising good agreement with the extrapolated values given in Table 1. Recent experimental determination of the inelastic mean free path of Ge at lower energies were published by Berényi et al. [15].

An alternative approach is to use mean free path values obtained in the literature for electron energy loss spectroscopy (EELS) and extrapolate these to smaller energies. Here a semi-empirical formula was proposed by Malis et al. [16]. It is intended for use in an electron microscope, where an aperture in front of the analyzer sets an upper limit β to the angular range of the detected electrons. This approximation gives for λ in nm and E in keV:

$$\lambda \approx \frac{106FE}{E_m \ln(2\beta E/E_m)} \tag{3}$$

with $E_m = 7.4Z^{0.36}$, and F a relativistic correction factor:

$$F = \frac{1 + (E/1022)}{(1 + (E/511))^2}.$$

In applications without aperture, we have to restrict the range of allowable β angles, as the underlying theory applies only in the dipole region. This limited range can be approximated roughly by replacing β by $\sqrt{E_p/E}$ [17]. In this way this approach gives values that are 15–25% smaller than the equation by Tanuma et al. [10].

The differential elastic cross-sections were obtained from the ELSEPA package written by Salvat et al. [12]. In these experiments we are starting to approach the Rutherford limit, where the differential cross-section is proportional to Z^2/E^2. In this limit the Ge cross-section is 28.4 times that of C.

2. Experimental details

Thin evaporated carbon films (supplied by Arizona Carbon Foil Company) with a nominal thickness of 8 μg/cm^2 were transferred on a shim with 2 mm holes. These samples were introduced into the electron momentum spectrometer, extensively described in Ref. [18]. The spectrometer was used in this work for elastic scattering. The carbon films were annealed to ensure is was conductive and to clean it from adsorbates. A 2 Å or 20 Å thick Ge layer was evaporated on this film (as judged from a crystal thickness monitor), the pressure during evaporation was in the 10^{-6} Pa range. After evaporation the sample was transferred under vacuum to the main chamber (pressure in the 10^{-9} Pa range). An electron beam of 0.2–1 nA

Table 1
The inelastic mean free path (calculated according to [10] and according to [11]), the differential cross-section for elastic scattering at 45° for C and Ge [12], at the energies used in this paper

E_0 (keV)	λ_{in} C (Å) [10]	λ_{in} C (Å) [11]	λ_{in} Ge (Å) [10]	λ_{in} Ge (Å) [11]	dσ/dΩ C 45° (Å^2)	dσ/dΩ Ge 45° (Å^2)	$d\sigma/d\Omega_{Ge}$:$d\sigma/d\Omega_C$
15	270	171	206	190	9.7×10^{-5}	2.3×10^{-3}	23:1
20	346	221	264	243	5.6×10^{-5}	1.4×10^{-3}	25:1
25	421	268	320	294	3.6×10^{-5}	0.96×10^{-3}	27:1
30	494	314	375	345	2.5×10^{-5}	0.70×10^{-3}	28:1

The last column shows the ratio of the differential elastic cross-section of Ge and C at 45°.

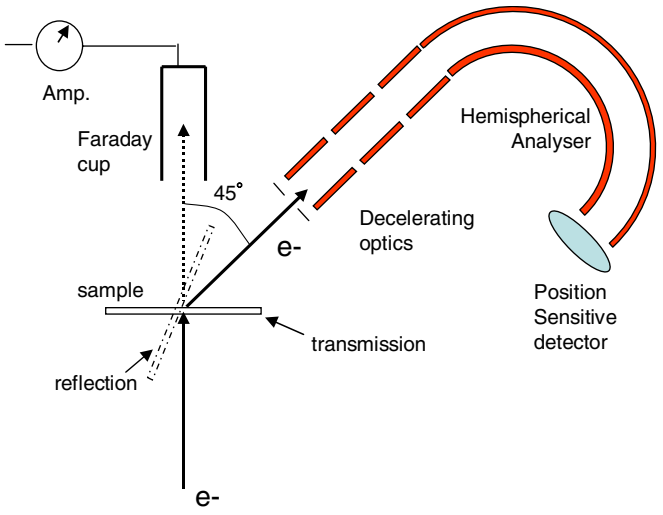

Fig. 1. Schematic view of the experiment.

impinged on the sample. The measurements were either done in a reflection geometry, or a transmission geometry. In both cases most of the beam was transmitted through the sample and collected in a Faraday cup behind the sample (see Fig. 1). The beam diameter (0.1 mm) is much smaller than the 2 mm holes. Even when we use a support shim with 0.3 mm holes we do not detect counts in the analyzers, if there is no film covering the holes. Hence we are confident that in this case, using 2 mm holes, no electrons scattered from the support shim are detected, even when we come in or out at a relatively glancing angle of 22.5°, as is sometimes the case in this experiment.

In order to get good energy resolution we used as a filament a barium oxide dispenser (supplied by Heatwave Labs Inc., model 311 M), operating at a very low heating current The pass energy of the analyzer was set to 200 eV. A spectrum was collected in about 1 h.

The performance of the spectrometer was tested using a self-supporting Au film. Due to its high Z (and hence large elastic scattering cross-section) spectra could be taken with an extremely low beam current (0.05 nA, rather than the 0.5–1.0 nA used for the measurements on Ge and C). The Au measurements were done at 0.58 A current heating the dispenser (the value used for all the other measurements of this paper), and at 0.49 and 0.70 A. These results are shown in Fig. 2. All peak shapes are asymmetric, the measurements taken with high-filament current more so than the low filament current one, and the Gaussian fit, shown in Fig. 2 is clearly *not* describing the data well. The temperature dependence suggest that the Maxwell–Boltzmann energy distribution of the emitted electrons is reflected in the shape of the elastic peak. The Gaussian fits have a full-width-half maximum of 0.35 eV at 0.7 A, 0.27 eV at 0.58 A and 0.22 eV for the 0.49 A measurement. We think that this reflects the spectrometer performance, and that the Doppler broadening due to the motion of the Au atoms is negligible, due to the large mass of Au (see Eq. (1)).

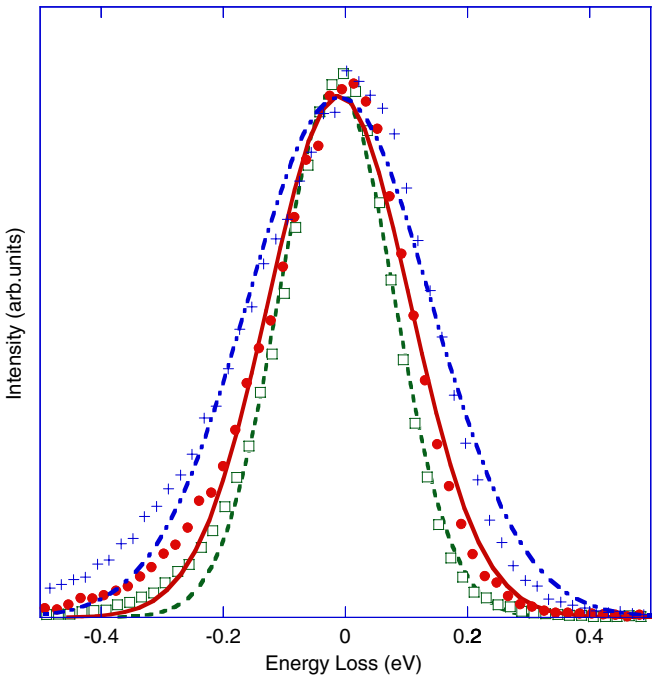

Fig. 2. Au elastic peak, taken at different filament currents (0.49 A: □, 0.58 A: ●, 0.70 A: +), and their Gaussian fit (dashed line, full line and dashed–dotted line, respectively). The asymmetry of the peak increases with filament current. This is thought to be due to the Maxwell–Boltzmann energy distribution of the emitted electrons.

Unfortunately the energy scale of our spectrometer is somewhat dependent on the sample position and filament conditions. Hence it is not possible to compare the energy positions of measurements that have the sample re-aligned (with 0.2 mm accuracy). The spectra were plotted in such a way that the position of the Carbon peak coincides with the prediction of Eq. (1). In practise the peak decomposition was always straight forward and the separation in energy ΔE of the C and Ge contribution was not affected by the uncertainty in the absolute energy scale.

3. Results

In the top panels of Fig. 3 we show the quasi-elastic peak of 30 keV electrons scattered from a 8 μg/cm^2 carbon film, both in transmission and in reflection. These peaks are much wider than the Au peaks shown in Fig. 2 (both are 0.8 eV FWHM), and this is due to the Doppler broadening. The peaks are fitted with a Gaussian and a Shirley background [19].

For an isotropic harmonically bound solid the momentum distribution is Gaussian, and the observed width is conveniently expressed in terms of the mean recoil energy $E_r = q^2/2M$ (0.81 eV for 30 keV electrons scattering from Carbon over 45°) and the mean kinetic energy of the atoms $\overline{E_k}$. The standard deviation σ of the observed Gaussian is given by [20]:

$$\sigma = \sqrt{\frac{4}{3}\overline{E_k}E_r}. \quad (4)$$

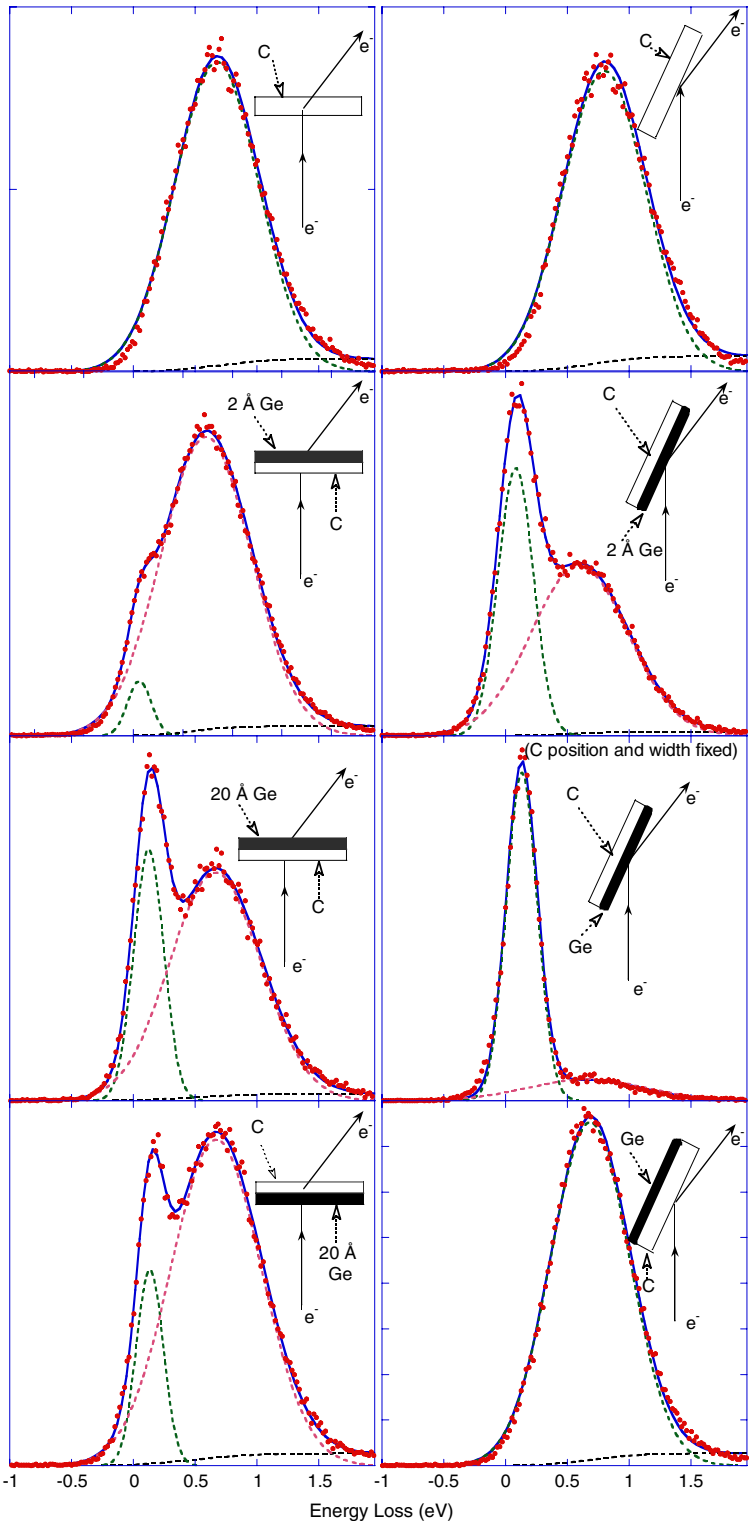

Fig. 3. The dependence of the elastic peak on the measurement geometry and Ge thickness. The carbon film thickness is 350 Å in all cases and the energy 30 keV. In the transmission experiment the incoming beam was along the surface normal, in the reflection measurement the angle between the surface normal and both the incoming and outgoing beam was 67.5°.

Using the mean kinetic energy for graphite of 108 meV as derived from neutron Compton scattering (NCS) [21] we obtain $\sigma = 0.34$ eV i.e. the full-width-half-maximum (FWHM) Γ is 0.79 eV, within the limits of error identical with our experimental estimate of 0.80 eV.

However, the Gaussian fit is not perfect, but in this case it is not due to the Maxwell–Boltzmann energy distribution of the emitted electrons, as this asymmetry is completely obscured by the large width of the carbon peak. Indeed the asymmetry for carbon peak is of opposite sign as that

observed for Au. A possible source of this deviation is a failure of the impulse approximation. In the derivation of Eq. (1) we assume that we scatter from a free particle. In reality the particle is part of the lattice. Possible consequences of this fact are discussed extensively in the neutron Compton literature, see for example [22]. It predicts that, due to the failure of the impulse approximation, the maximum will shift to slightly lower energy loss values, and the onset of the peak at the low energy loss side to be sharper than the decline at the high energy loss side. The latter observation is consistent with the deficiencies of the Gaussian fit. The fitting parameters obtained for the C spectra, and those obtained after Ge deposition are summarized in Table 3.

Now we deposit 2 ± 1 Å of Ge on the carbon film. We measure again a reflection and a transmission spectrum, in both cases the side of the film on which the Ge is deposited faces the analyzer. In spite of the thin deposited Ge film there is a clear difference in the shape of the elastic peak (second pair of spectra, Fig. 3). In the transmission case there is a distinct shoulder on the high energy side. For the reflection case there is a large peak at the same energy as the shoulder in the transmission case. We will assume that these new peaks are due to germanium. Peak positions were obtained from a two-component fit plus a Shirley background. The Ge peak is considerable sharper than the C peak, and its width is indeed very similar to the width of the Au peak taken with the same filament current. The separation of Ge and C peak was calculated using Eq. (1) and this is compared in Table 2 with the experimentally obtained separation. The separation seems to be systematically 0.1 eV smaller than the calculated one. Again this is consistent with a noticeable shift of the C peak to lower energy loss values, due to a failure of the impulse approximation.

The small amount of germanium is easily observed, as its cross-section for elastic scattering is much larger than that of carbon (see Table 1). Indeed, for very thin Ge and C films, much thinner than the inelastic mean free path, the areas of the components is expected to be proportional to the number of atoms per unit area times the differential elastic cross-section. The fact that the relative intensity of the Ge component is much larger for the reflection geometry compared to the transmission geometry indicates that the effective probing depth in the first case is much less than 350 Å, the thickness of the carbon film. In the transmission case the whole film contributes (although the side facing the analyzer a bit more than the other side, as we will see later).

Additional deposition of 18 ± 2 Å of Ge (total nominal thickness is now 20 Å) results in a Ge peak that is higher than the C peak in the transmission case. In the reflection case the C peak is reduced to just a tail at the high energy-loss side of the Ge peak (third pair of spectra, Fig. 3).

Clearly the amount of Ge observed depends on the measurement geometry. This is confirmed by spinning the sample over 180° and measuring the samples with a 20 Å Ge layer again. Now the Ge peak height is reduced significantly in the transmission geometry, and disappears below the detection limit in the reflection geometry.

For the transmission geometry with 20 Å Ge at the exit side we studied the energy dependence of the shape of the elastic peak. The results are shown in Fig. 4 and Table 3. Clearly the separation of the Ge and C peak becomes less with decreasing energy, and the peak decomposition and peak width determination becomes more and more questionable with decreasing energy.

To get more information about the selective attenuation of the elastic peak signals as a function of measurement geometry, we prepared a new sample, again 8 μg/cm^2 (≃350 Å thick) carbon film with a 20 Å Ge layer deposited on this. We now do transmission measurements, again for 30 keV electrons, but vary the angle of the electron beam as indicated in the inserts in Fig. 5. The spectra (a–f) are ordered in such a way that the relative intensity of the Ge peak increases. In the case (a–c) the carbon layer is facing the analyzer, in case (d–f) the Ge layer is facing the analyzer. Spectrum (c) and (d) are almost identical. Spectrum (b) and (d) are taken in the same geometry, and for nominally the same sample composition as the two spectra in the bottom of the left column of Fig. 3. Indeed the shape of these spectra are almost identical. The fit results are summarized again in Table 4.

Table 2
The energy separation ΔE and peak width, as obtained from the fitting procedure, for the various geometries, shown in Fig. 3

Configuration	Ge (Å)	ΔE observed (eV)	FWHM Ge (eV)	FWHM C (eV)	Ratio observed A_{Ge}/A_C	Ratio calculated A_{Ge}/A_C [10]	Ratio calculated A_{Ge}/A_C [11]
C only transmission	0.0	–	–	0.80	–	–	
C only reflection	0.0	–	–	0.79	–	–	
Ge at exit transmission	2	0.54	0.22	0.85	0.044	0.07	0.08
Ge side reflection	2	0.52	0.33	0.92	0.56	0.23	0.36
Ge at exit transmission	20	0.54	0.29	0.86	0.36	0.73	0.79
Ge side reflection	20	(0.54)	0.30	(0.87)	5.7	2.7	4.2
C at exit transmission	20	0.54	0.26	0.85	0.17	0.53	0.48
C side reflection	20	–	–	0.74	<0.03	0.05	0.009

A_{Ge}/A_C is the Ge peak area divided by the C peak area. Values in brackets were kept fixed in the fitting procedure. The theoretical ΔE value, according to Eq. (1) is 0.66 eV for 30 keV electrons. The calculated intensity ratios, shown in the last two columns use the mean free path as given by [10] or [11] respectively.

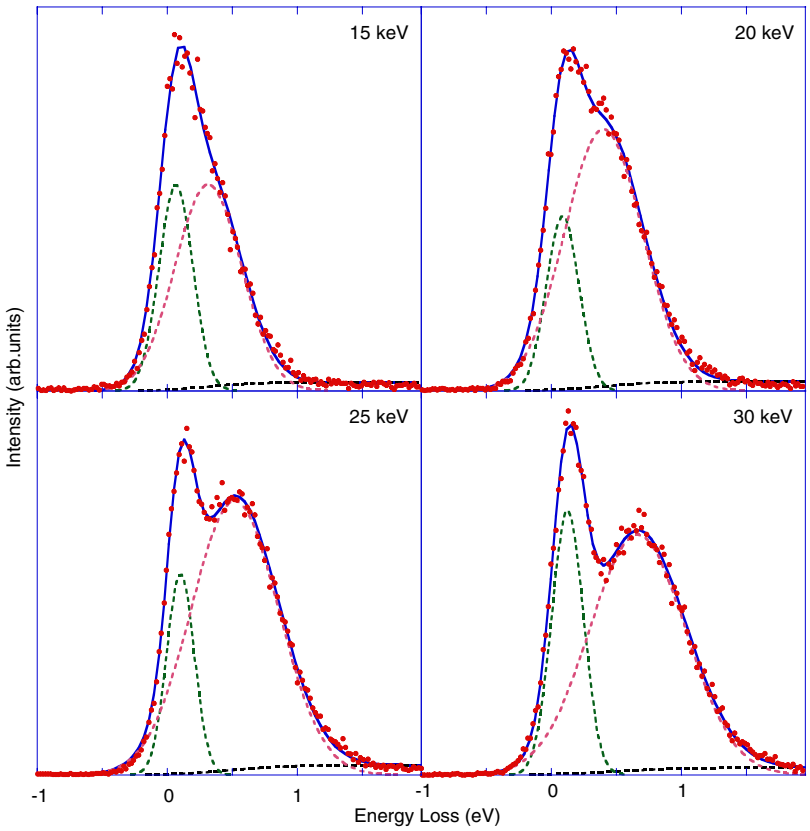

Fig. 4. The dependence of the elastic peak on the energy of the incoming electrons, measured in transmission for a carbon film with 20 Å of Ge on the exit side.

Table 3
The calculated and observed energy splitting, σ and area ratio as obtained from the fit for various incoming electron energies for the data shown in Fig. 4

E_0 (keV)	ΔE calculated (eV)	ΔE observed (eV)	FWHM Ge (eV)	FWHM C (eV)	Ratio A_{Ge}/A_C
15	0.33	0.25	0.31	0.59	0.51
20	0.44	0.31	0.31	0.71	0.27
25	0.55	0.41	0.26	0.80	0.22
30	0.66	0.54	0.28	0.84	0.36

4. Discussion

We used a carbon film with density of 8 μg/cm^2. In situ we evaporated 20 Å of Ge (as judged from a crystal thickness monitor) on this free standing film, corresponding to a density of $5.32 \times 20 \times 10^{-8} = 1.06$ μg/cm^2. Thus the ratio of the number of Ge atoms per cm^{-2} to the number of C atoms per cm^{-2} is N_{Ge}:$N_C = (1.06/m_{Ge})$:$(8/m_C) = 1$:45.2. The differential cross-section ratio varies from 23:1 at 15 keV to 28:1 at 30 keV. If attenuation effects (due to inelastic energy loss events, which reduce the number of counts in the elastic peak, for both C and Ge) could be neglected we would thus expect the Ge:C peak area to be 1:1.61 at 30 keV. The wildly varying peak areas observed demonstrate clearly that attenuation effects are very important indeed.

In order to get some quantitative insight we will now try to calculate the elastic peak area ratio for the spectra shown in Figs. 3 and 5. We assume that each detected electron has been scattered in a single collision over 45°. The thickness of the Ge and C layer is t_{Ge} and t_C respectively. The probability that an electron is deflected over 45° at a certain depth τ is proportional to the differential elastic cross-section of the atom at that depth times the number of atoms per unit volume. However, this electron will only contribute to the elastic peak if it is not scattered inelastically, before or after the deflection. Hence we have to consider the length of the trajectories, as is illustrated in Fig. 6.

Consider first the case of the deflection occurring in the first layer, referred to in the following as layer a, at depth τ, $\tau < t_a$. The length of the trajectory in layer a is $l_a = \tau/\cos(\theta_{in}) + (t_a - \tau)/\cos(\theta_{out})$. The length in layer b is $l_b = t_b/\cos(\theta_{out})$. The probability $P(\tau)$ that an electron from an elastic scattering event at depth τ reaches the detector without energy loss is then: $P(\tau) = \exp -l_a/\lambda_a \exp -l_b/\lambda_b$. Similar expressions can be derived for scattering in the second layer, layer b.

The intensity due to layer a is thus proportional to

$$I_a = C\rho_a \left(\frac{d\sigma}{d\Omega}(45^\circ)\right)_a \int_0^{t_a} P(\tau)d\tau, \quad (5)$$

and similarly for layer b:

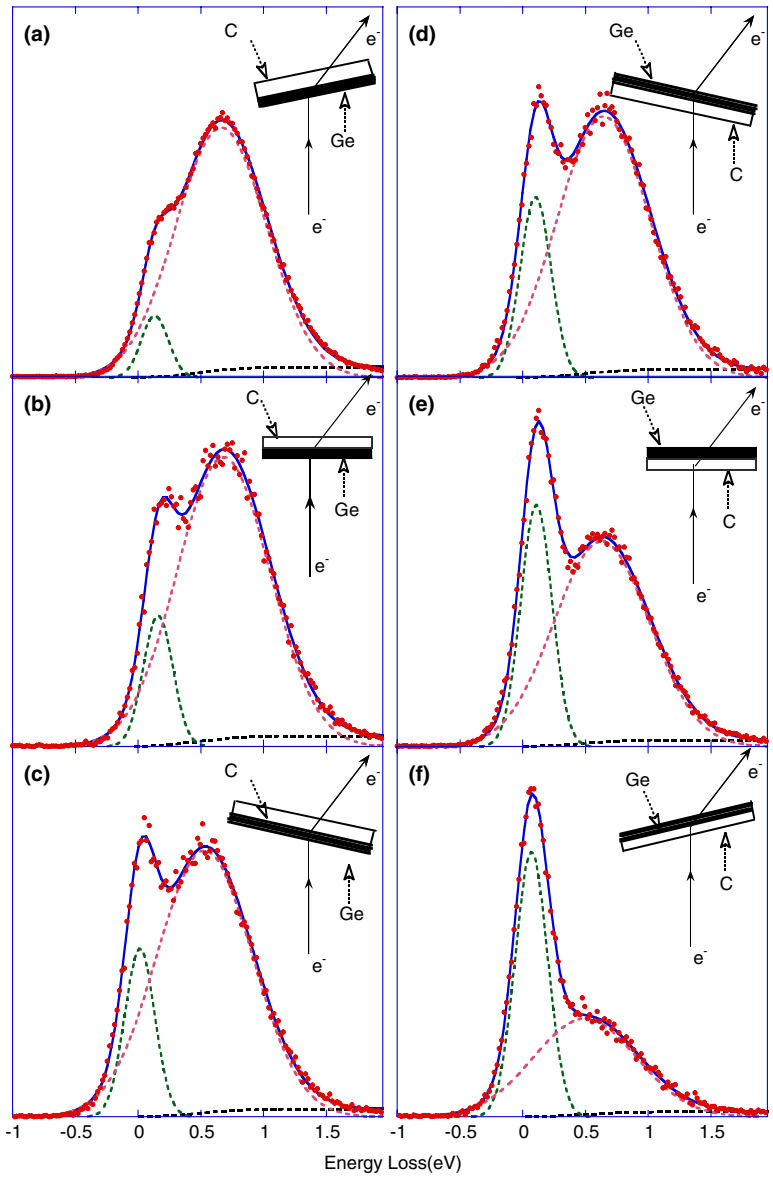

Fig. 5. The measured spectra as a function of sample angle. Spectra are taken with the incoming beam making an angle θ with the surface normal of 22.5° (case a and f), 0° (case b and e) and −22.5° (case c and d). The geometry is sketched as an insert in each plot.

Table 4
The various quantities as obtained from the fitting procedure for the various geometries, shown in Fig. 5

Configuration	Θ (deg)	ΔE observed (eV)	FWHM Ge (eV)	FWHM C (eV)	Ratio observed A_{Ge}/A_C	Ratio calculated A_{Ge}/A_C [10]	Ratio calculated A_{Ge}/A_C [11]
C at exit	22.5	0.53	0.25	0.84	0.09	0.33	0.23
C at exit	0.0	0.52	0.28	0.87	0.14	0.53	0.48
C at exit	−22.5	0.51	0.28	0.89	0.20	0.62	0.62
Ge at exit	−22.5	0.54	0.29	0.87	0.23	0.62	0.62
Ge at exit	0.0	0.52	0.29	0.89	0.38	0.73	0.79
Ge at exit	22.5	(0.53)	0.33	0.85	1.2	1.06	1.36

Further as Table 2.

$$I_b = C\rho_b\left(\frac{d\sigma}{d\Omega}(45^\circ)\right)_b \int_{t_a}^{t_a+t_b} P(\tau)d\tau \qquad (6)$$

with $\rho_{a,b}$ the number of atoms per unit volume. Thus the ratio of the peak intensities can be obtained by numerical integration using the nominally known thicknesses and cross-sections. This procedure can be modified somewhat for the reflection geometry. Here the intensity of elastically scattered electrons in the surface layer is not affected by inelastic scattering in the substrate, but the intensity of

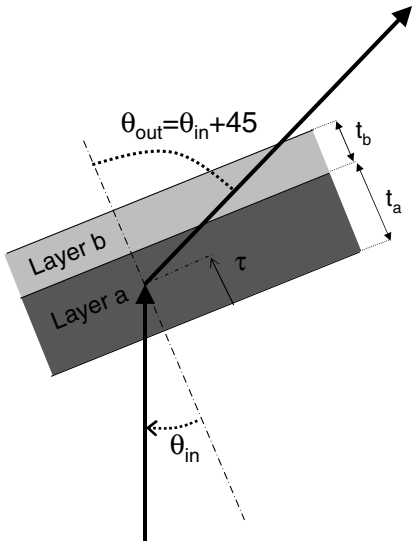

Fig. 6. Schematic drawing of the path lengths in a two-layer target.

elastically scattered electrons in the substrate is influenced by inelastic scattering in both surface and substrate layer. The calculated results are given as well in Tables 2 and 4. Generally there is a poor agreement with the experiment. For transmission measurements the calculated Ge/C intensity ratio is about a factor of three larger than the observed one, whereas in reflection measurements it is the other way around.

There is one special case. If $\theta_{in} = -22.5°$ then for our scattering geometry, $\cos\theta_{in} = \cos\theta_{out}$ and the path length through either layer a or b is independent from the depth, (and even in which layer) the elastic deflection occurs. Hence the attenuation is the same, independent of depth and the element one scattered from. The observed peak areas should then relate simply as

$$A_{Ge} : A_C = N_{Ge}\left(\frac{d\sigma}{d\Omega}(45°)\right)_{Ge} : N_C\left(\frac{d\sigma}{d\Omega}(45°)\right)_C. \quad (7)$$

Thus for this angle it should not matter which element faces the analyzer, or what is the value of the inelastic mean free path in either layer. Experimentally the similarity of case (c) and (d) in Fig. 5 confirm this observation. This is an important fact. Assuming that the differential cross-section is known we can determine at $\theta_{in} = -22.5$ the ratio of the number of Ge and C atoms in the film. Subsequently by rotating away from $-22.5°$ we can determine uniquely the thickness and order of the two layers. Alternatively, if the thickness of both layers is known, we can use the same procedure to determine both the differential elastic scattering cross-section and the inelastic mean free path in both layers.

5. Summary and conclusion

We have demonstrated that at high energy resolution the peaks of electrons scattered from heavy and light elements (in particular carbon and germanium) can be separated. At relatively low energies of 15–20 keV the separation is not complete, but especially at the highest energy (30 keV) the decomposition of the measured signal is quite unambiguous. By changing the measurement geometry large differences are observed in the intensity of the Ge and C peak, much larger than expectations, based on a naive model and using mean free path taken from the XPS literature or EELS literature.

Our interpretation is based on a single scattering approximation. This approximation is known from Monte Carlo simulations to be poor for heavy elements and at low energies but should become quite reasonable at the energies considered in this paper [23].

We have thus demonstrated here that quasi-elastic electron scattering spectra, taken at high-resolution contains at least qualitatively, interpretable information about the thin film composition, both in reflection and transmission. This technique shares some aspects of Rutherford back scattering (scattering of particles of the potential of a nucleus) and electron spectroscopy (information is contained in the signal of those electrons that have not scattered inelastically). The first characteristic is favorable for a quantitative interpretation of the data, whereas the second characteristic makes the technique surface sensitive. The combination of these two characteristics is quite unique and makes this technique of interest for quantitative surface analysis or electron microscopy. The probing depth is larger than in XPS or Auger spectroscopy due to the high energy of the electrons involved.

However there are also clear limitations. Currently we can only separate the lightest elements (up to, say, carbon) from heavy ones. Spectrometers operating at higher momentum transfer could in principle separate more elements, and the separation of, for example, Si and Ge could be accomplished by a 30 keV spectrometer with similar energy resolution, but a scattering angle of 135° (separation more than 1 eV, a larger beam current would be required due to the reduced cross-section). Also this technique is suitable for detecting small quantities of heavy elements in a low-Z matrix, but the other way around is not possible, due to the approximate increase of the cross-section with Z^2.

The relative small beam current required (<1 nA) would allow for the use of field emitters, making it possible to collect spectra from small areas. The fact that this technique uses high-energy electrons makes integration in an electron microscope attractive, in particular in a scanning electron microscope, where it is straight-forward to measure electrons scattered over large angles.

The disappointing agreement between the calculated and observed intensity ratio can be attributed to deviation of the sample structure from the assumed one (wrong Ge layer thickness, islanding of the Ge overlayer), uncertainties in the inelastic mane free path, failure of the single scattering approach and uncertainties in the peak decomposition, influences of surface/interface plasmons neglected in our analysis. The influence of the latter is expected to be small at these high electron energies [24]. We plan to

investigate this further by making samples suitable for ion beam and electron microscope analysis, and further increasing the energy of the incoming electrons. The validity of the single scattering approximation can be studied using Monte Carlo simulations. Once fully understood this method will be very helpful in sample characterization, or, for samples with known morphology an accurate way of determining the inelastic mean free path. Note that there is a large redundancy in the data. It is, for example, impossible to obtain a good fit for both transmission and glancing spectra by treating the Ge thickness as a fitting parameter. The glancing spectra seem to suggest that the Ge thickness is too large, whereas the transmission spectra generally seem to indicate that the Ge thickness is too small.

Acknowledgements

This research was made possible by a grant of the Australian Research Council. The authors want to thank Erich Weigold for critically reading the manuscript.

References

[1] G. Gergely, Progress Surf. Sci. 71 (2002) 31.
[2] W.S.M. Werner, Surf. Interf. Anal. 31 (2001) 141.
[3] W.S.M. Werner, C. Tomastik, T. Cabela, G. Richter, H. Stri, J. Electron Spectrosc. Relat. Phenom. 113 (2001) 127.
[4] H. Boersch, R. Wolter, H. Schoenebeck, Z. Physik 199 (1967) 124.
[5] D. Varga, K. Tökesi, Z. Berènyi, J. Tóth, L. Körvér, G. Gergely, A. Sulyok, Surf. Interf. Anal. 31 (2001) 1019.
[6] G.T. Orosz, G. Gergely, M. Menyhard, J. Tóth, D. Varga, B. Lesiak, A. Jablonski, Surf. Sci. 566–568 (2004) 544.
[7] M. Vos, Phys. Rev. A 65 (2002) 12703.
[8] C.A. Chatzidimitriou-Dreismann, M. Vos, C. Kleiner, T. Abdul-Redah, Phys. Rev. Lett. 91 (2003) 57403.
[9] M. Vos, C. Chatzidimitriou-Dreismann, T. Abdul-Redah, J. Mayers, Nucl. Inst. Methods B 227 (2004) 233.
[10] S. Tanuma, C.J. Powell, D.R. Penn, Surf. Interf. Anal. 20 (1993) 77.
[11] S. Tanuma, C.J. Powell, D.R. Penn, Surf. Interf. Anal. 37 (2005) 1.
[12] F. Salvat, A. Jablonski, C.J. Powell, Compu. Phys. Commun. 165 (2005) 157.
[13] J. Zemek, J. Potmesil, M. Vanecek, B. Lesiak, A. Jablonski, Appl. Phys. Lett. 87 (26) (2005) 262114.
[14] D.L. Misell, R.A. Crick, J. Phys. C: Solid State Phys. 4 (12) (1971) 1591.
[15] Z. Berényi, B. Aszálos-Kiss, J. Tóth, D. Varga, L. Köver, K. Tökési, I. Cserny, S. Tanuma, Surf. Sci. 566–568 (Part 2) (2004) 1174.
[16] T. Malis, S. Cheng, R. Egerton, J. Electron Micros. Technol. 8 (1988) 193.
[17] R.F. Egerton, private communication.
[18] M. Vos, G.P. Cornish, E. Weigold, Rev. Sci. Instrum. 71 (2000) 3831.
[19] D.A. Shirley, Phys. Rev. B 5 (1972) 4709.
[20] M.P. Paoli, R.S. Holt, J. Phys. C: Solid State Phys. 21 (1988) 3633.
[21] J. Mayers, T.M. Burke, R.J. Newport, J. Phys.: Condens. Matter 6 (1994) 641.
[22] G.I. Watson, J. Phys.: Condens. Matter 8 (1996) 5955.
[23] A. Jablonski, C. Powell, Surf. Sci. 551 (2004) 106.
[24] W.S.M. Werner, Surf. Sci. 526 (2003) L159.